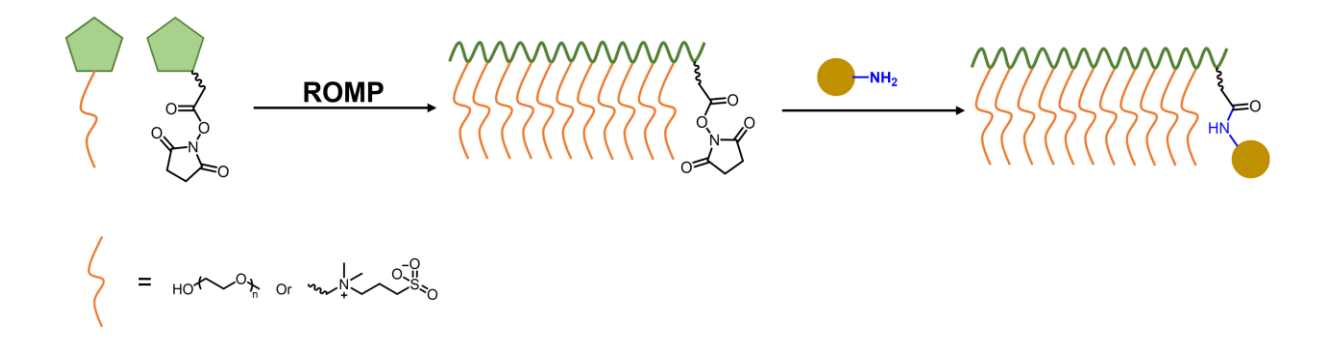
Poly(oxanorbornene)-Protein Conjugates Prepared by Grafting-to ROMP as Alternatives for PEG

Elizabathe Davis¹, Adam A. Caparco¹, Nicole F. Steinmetz^{1,2,3,4,5,6}, Jonathan K. Pokorski*^{1,2,3}

- ¹Department of NanoEngineering, University of California, San Diego, La Jolla, CA 92093, USA
- ²Center for Nano-ImmunoEngineering, University of California, San Diego, La Jolla, CA 92093, USA
- ³Institute for Materials Discovery and Design, University of California, San Diego, La Jolla, CA 92093, USA
- ⁴Department of Bioengineering, University of California, San Diego, La Jolla, CA 92093, USA
- ⁵Department of Radiology, University of California, San Diego, La Jolla, CA 92093, USA ⁶Moores Cancer Center, University of California, San Diego, La Jolla, CA 92093, USA

ABSTRACT



PEGylation is the gold standard in protein-polymer conjugation, improving circulation half-life of biologics while mitigating the immune response to a foreign substance. However, pre-existing anti-PEG antibodies in healthy humans are becoming increasingly prevalent and elicitation of anti-PEG antibodies when patients are administered with PEGylated therapeutics challenges their safety profile. In our current study, two distinct amine-

reactive poly(oxanorbornene) (PONB) imide-based water-soluble block co-polymers were synthesized using ring opening metathesis polymerization (ROMP). The synthesized block-copolymers include PEG-based PONB-PEG and sulfobetaine-based PONB-Zwit. The polymers were then covalently conjugated to amine residues of lysozyme (Lyz) and urate oxidase (UO) using a grafting-to bioconjugation technique. Both Lyz-PONB and UO-PONB conjugates retained significant bioactivities after bioconjugation. Immune recognition studies of UO-PONB conjugates indicated comparable lowering of protein immunogenicity when compared to PEGylated UO. PEG-specific immune recognition was negligible for UO-PONB-Zwit conjugates, as expected. These polymers provide a new alternative for PEG-based systems that retain high levels of activity for the biologic while showing improved immune recognition profiles.

INTRODUCTION

The covalent conjugation of polyethylene glycol (PEG) to therapeutic proteins or PEGylation has been the gold standard in protein bioconjugation since its advent in 1977.^{1,2} More than 24 PEGylated proteins have been approved by the FDA for various diseases like cancer, hepatitis and rheumatoid arthritis since 1990.^{3–5} PEGylation reduces the immunogenicity, while increasing protein stability and blood circulation half-life of the native protein.^{6–8} However, there is an increasing prevalence of anti-PEG antibodies in the population and administration of PEGylated therapies can further elicit anti-PEG immune responses.^{9–13} The occurrence of pre-existing anti-PEG in healthy human subjects increased from 0.2% according to a study in 1984 to more than 44% as reported in 2016.^{14,15} Such an increase can be attributed to the rising exposure of the populace to PEG in daily use products. The presence of pre-existing anti-PEG causes effects such as

loss of protein activity, accelerated blood clearance (ABC), and reduces the safety of PEGylated therapeutics. 16–18 Additionally, this could also lead to serious allergic and hypersensitivity reactions in patients receiving PEGylated protein therapeutics. 16,19

The presence of anti-PEG in patients has led to several PEGylated therapeutics facing challenges in clinical studies. For instance, PEGinesatide (OMONTYS®), used for the treatment of anemia, was withdrawn soon after FDA approval in 2012 due to fatal hypersensitivity reactions.²⁰ The clinical trials of PEGnivacogin were terminated as patients developed serious allergic reactions due to pre-existing anti-PEG antibodies.¹⁸ Also, the clinical trials of Pegloticase (PEG-uricase or KRYSTEXXA®) revealed loss of treatment response, increased drug clearance, risk of infusion reactions and adverse events in patients due to pre-existing anti-PEG antibodies.^{21,22} Thus, there has been great interest in studying potential PEG alternatives in bioconjugation and protein therapeutics in the past two decades.^{23–29}

Advances in polymer chemistry and the development of controlled polymerization techniques like atom transfer radical polymerization, reversible addition fragmentation polymerization, nitroxide mediated polymerization and ring opening metathesis polymerization (ROMP) have enabled the synthesis of well-defined multifunctional systems with low dispersity (Đ), a variety of end-group functionalities, and architectures.^{30–37} A wide variety of water-soluble polymer alternatives to PEG have been reported and are primarily derived from acrylate or acrylamide monomers, although others have been investigated, as well.^{23,24,27,38–45}

Among these PEG alternatives, the PEG-based brush polymer, poly(oligo(ethylene glycol) methyl ether methacrylate) (POEGMA), synthesized by controlled radical

polymerization techniques has been extensively studied and POEGMA-protein conjugates show similar or improved pharmacokinetics and pharmacodynamics compared to their linear PEG counterparts. 46–52 In addition, POEGMA with up to nine ethylene glycol repeat units significantly diminished recognition by anti-PEG antibodies when compared to high molecular weight linear PEG. 48,49 Superhydrophilic zwitterionic polymers are an additional promising class of polymer that are antifouling and protein conjugates derived from these polymers do not elicit any polymer specific antibodies while maintaining high protein activity leading to superior pharmacokinetics. 53–57 Owing to the potential of zwitterionic polymers and PEG-based brush polymers in improving immunogenic behavior while evading polymer specific antigenicity, the utility of zwitterionic and PEG-based polynorbornene (**PNB**) polymers in bioconjugation has been an ongoing area of inquiry.

Recent studies from our lab demonstrated improved immune shielding of proteins by **PNB** based polymers in protein-polymer conjugates.^{58–60} Herein, we describe the advantages of poly(oxanorbornene) (**PONB**) based water soluble polymers as PEG alternatives for protein conjugation and demonstrate potential utility in a therapeutic protein. **PONB** polymers offer a unique solution relative to **PNB**, since the backbone oxygen increases polarity and may impact polymer conformation and solubility. We recently reported a grafting-from synthesis of **PNBs**, however, **PONBs** were synthetically inaccessible due to limitations in our aqueous catalyst system, requiring a grafting-to procedure.

This study reports the synthesis of **PONB** based conjugates of **Lyz** and the therapeutically relevant enzyme, urate oxidase (**UO**) or uricase by a grafting-to ROMP bioconjugation method. **Lyz** is a well-studied protein available in large quantities and is thus widely used

as a model protein. **UO** is involved in the regulation of uric acid (**UA**) formation and deposition in joints and tissues by degrading into allantoin which can be excreted from the body. 61–66 Enzymatic replacement of **UO** is a common gout treatment and, as mentioned previously, PEGylation of **UO** led to significant adverse events in treatment. Here we present a PEG alternative with high retained enzymatic activity and low immune recognition against the protein and the conjugated polymer.

RESULTS AND DISCUSSION

Synthesis of PONB-based block co-polymers. Two types of oxanorbornene (oNB) derivatives were used as monomers: oNB-PEG is a PEG-based monomer with a mPEG-350 side chain and oNB-Zwit contains a zwitterionic sulfobetaine side chain.^{67,68} Grubb's 3rd generation catalyst (G3) was used to initiate the ROMP polymerization of oNB-PEG and oNB-Zwit monomers to obtain polymers, PONB-PEG and PONB-Zwit, respectively (Figure 1A). Polymer molecular weights of 5, 10, 20 kDa for both PONB-PEG and PONB-Zwit polymers were targeted as most FDA approved protein therapeutics are conjugated to PEG polymers of molecular weight ranging from 5 to 20 kDa. The polymers were made to be reactive by introducing a small block of norbornene monomer with a *N*-succinimidyl ester functionality (NB-NHS) at the chain end before terminating with ethyl vinyl ether (EVE). The NB-NHS block in the polymer chain end, facilitated covalent conjugation of the polymers to amine functionalities of proteins.

The successful synthesis of **PONB-PEG** polymers was confirmed by ¹H nuclear magnetic resonance (¹H NMR) (**Figure S1, S3, S4**) and gel permeation chromatography (GPC) (**Figure 1B**). ¹H NMR of the crude **5-PONB-PEG** indicated that the vinylic monomer peaks of **oNB-PEG** at 6.5 ppm and 5.23 ppm, (**a**) had disappeared and new broad peaks

corresponding to vinylic protons of the polymer backbone appeared at 6 and 5.76 ppm (d) (Figure S1). The peak at 2.8 ppm corresponds to the *N*-succinimidyl moiety and confirmed the successful incorporation of **NB-NHS** monomers at the polymer chain end of all the **PONB-PEG** polymers (Figure S1, S3, and S4). The integration of peaks corresponding to the phenyl end group (c) and *N*-succinimidyl moiety (e) indicates that 5-**PONB-PEG** co-polymers had an average of 4 **NB-NHS** monomer units per polymer chain (**Figure S2**). The molecular weights (Mn, Mw) and dispersity (Đ) of the synthesized polymers were obtained from GPC. Targeted molecular weights were attained for all the **PONB-PEG** polymers (**Figure 1B**) and dispersity values (Đ = 1.07-1.16) indicated controlled polymerization. The development of small shoulder peaks was observed in the chromatograms as the molecular weight of the polymers increased, which could be attributed to chain-transfer reactions.³³

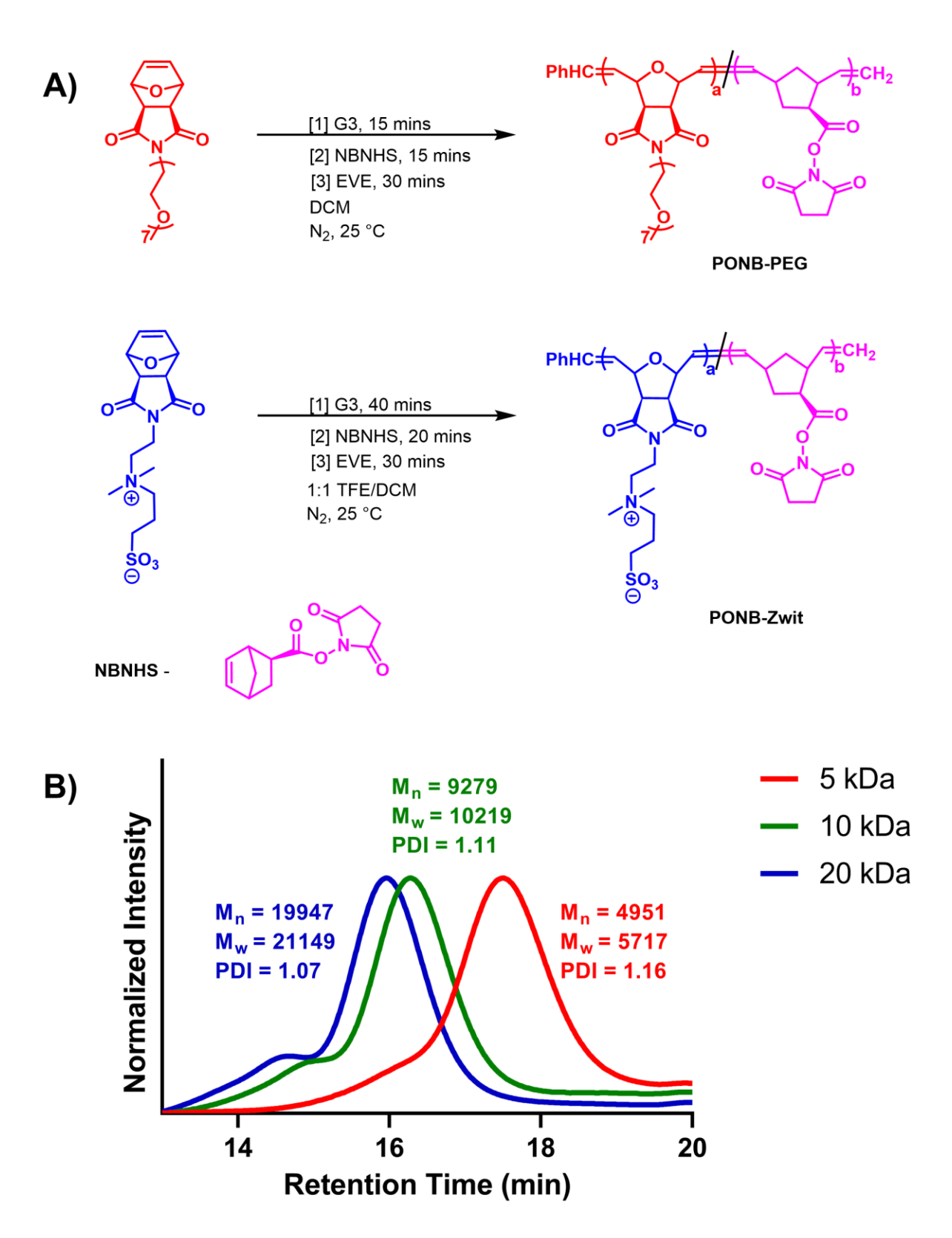


Figure 1. **A)** Synthetic scheme of **PONB-PEG** and **PONB-Zwit** co-polymers **B)** GPC traces of **PONB-PEG** polymers. Molecular weights of 5, 10 and 20 kDa were targeted.

The **PONB-Zwit** co-polymers were characterized by aqueous GPC, ¹H NMR and matrixassisted laser desorption/ionization-time of flight (MALDI-TOF) mass spectrometry (MS). However, the aqueous GPC of PONB-Zwit polymers generated unreliable data, as we have seen previously. Several potential reasons could contribute to this; the polymer standards used for calibration are poor equivalents, interactions of the polymer with column material lead to broadening and inaccurate retention, and aggregation and poor solubility of the polymers in the eluent. 67,69,70 Therefore, molecular weights (Mn) of the **PONB-Zwit** co-polymers were determined by end-group analysis by ¹H NMR (**Figure** 2).71 The integration value of the phenyl end group (a) was compared with the protons of the unsaturated backbone (c, c'). The end-group analysis of PONB-Zwit with targeted molecular weight of 5 kDa indicated an Mn of 5.02 kDa. MALDI-TOF MS analysis (Figure **S6**) of the same polymer was in agreement and indicated a M_n of 6.6 kDa and a gaussian distribution of molecular weights confirmed the successful synthesis of targeted molecular weight with a low Đ (< 1.3).^{72,73} The end-group analysis by ¹H NMR and mass analysis by MALDI-TOF MS of **PONB-Zwit** block co-polymers targeted for 10 and 20 kDa did not provide useful data which is due to low resolution at higher molecular weights and potential mass discrimination.⁷⁴ However, ¹H NMR of polymerization of **PONB-Zwit** polymers show the complete consumption of monomer peaks (Figure S7) and SDS-PAGE (Figure \$10) of polymers showed a steady decrease in electrophoretic mobility as the polymer size increased, indicating that the targeted molecular weights were likely

achieved. The peak at 2.8 ppm indicative of **NBNHS** incorporation in the polymer chain end was masked by peak corresponding to the polymer but was evident from the successful conjugation to proteins that followed (**Figure S8**, **S9**).

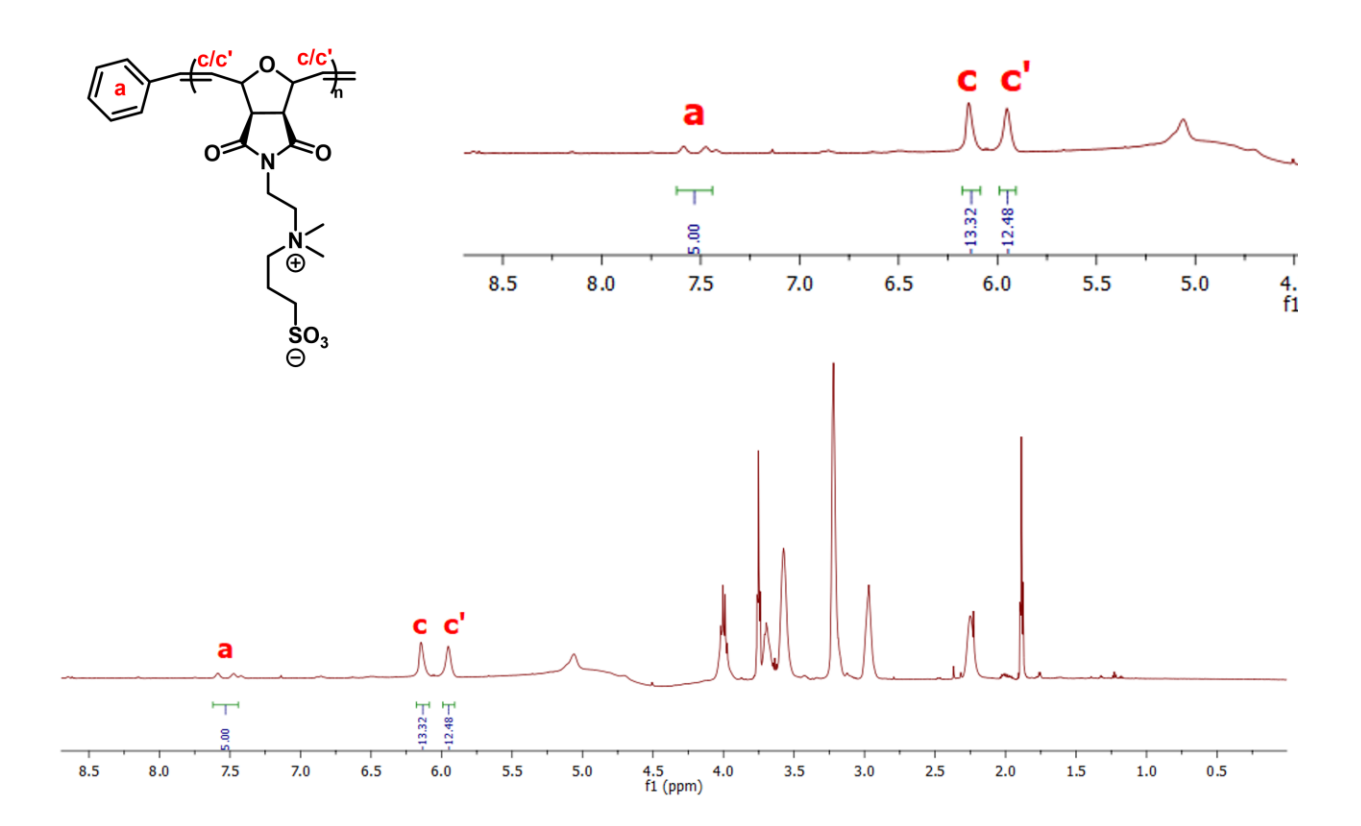


Figure 2. End-group analysis of PONB-Zwit polymer.

The spectrum indicates ¹H NMR of a PONB-Zwit polymer with 5 kDa targeted molecular weight. The protons of phenyl end-group and the protons of unsaturated backbone are indicated as **a** and **c/c'** respectively (**c**- trans, **c'**- cis)

Synthesis of grafting-to lysozyme conjugates, Lyz-PONB. PONB-PEG and PONB-Zwit block co-polymers were conjugated to Lyz, targeting lysine residues on the surface (7 lysine residues, 6 solvent accessible) (Scheme 1). ~10 equivalents of either PONB-

PEG or PONB-Zwit relative to each lysine residues of Lyz was used for grafting-to conjugation and conjugates were further purified by fast protein liquid chromatography (FPLC). The conjugates eluted at retention volumes of 7-10 mL, while unreacted Lyz eluted at ~20 mL. Furthermore, the purified Lyz-PONB conjugates were characterized by sodium dodecyl sulfate—polyacrylamide gel electrophoresis (SDS-PAGE) (Figure 3B and 3D) and FPLC (Figure 3A and 3C). The extent of protein modification was determined by quantifying free amino groups using 2,4,6-trinitrobenzene sulfonic acid (TNBS) (Table S1).⁷⁵ All the conjugations resulted in a decrease in free amino groups compared to Lyz. A decrease in the degree of modification was observed in Lyz-PONB-Zwit conjugates with an increase in molecular weight of polymers.

Scheme 1: Synthesis of grafting-to PONB conjugates derived from Lyz.

Protein bands in the PAGE gel were visualized by Coomassie blue stain and showed broad bands (Lanes 3-5) with lower mobility indicating higher molecular weights compared to Lyz, confirming successful conjugation of the polymers (Figure 3B and 3D). Also, the mobilities of the Lyz-PONB conjugate bands decreased with an increase in molecular weight of the PONB polymers as expected for the formation of larger conjugates. The SDS-PAGE of Lyz-5 PONB-Zwit showed band at similar molecular

weights of Lyz, indicating similar electrophoretic mobilities of protein and protein-polymer conjugate (Figure 3D, Lane 3). In addition to Coomassie blue staining, Lyz-PONB-PEG conjugates were stained with iodine solution (Figure S11). Iodine staining is specific for PEG polymers and helps to visualize bioconjugates with PEG components. RDS-PAGE of all the Lyz-PONB conjugates following purification showed the absence of unreacted Lyz corroborated by the absence of elution at 20 mL in FPLC. In contrast to the unimodal peaks observed with Lyz-PONB-PEG conjugates, Lyz-PONB-Zwit conjugates, particularly Lyz-5 PONB-Zwit and Lyz-20 PONB-Zwit, exhibited multimodal conjugate peaks. This may be attributed to the formation of conjugates with differing grafting densities. Furthermore, in the SDS-PAGE analysis of Lyz-5 PONB-Zwit and Lyz-20 PONB-Zwit, lighter streaking at significantly higher molecular weights was observed, indicating the presence of small amounts of conjugates with potentially much higher grafting densities.

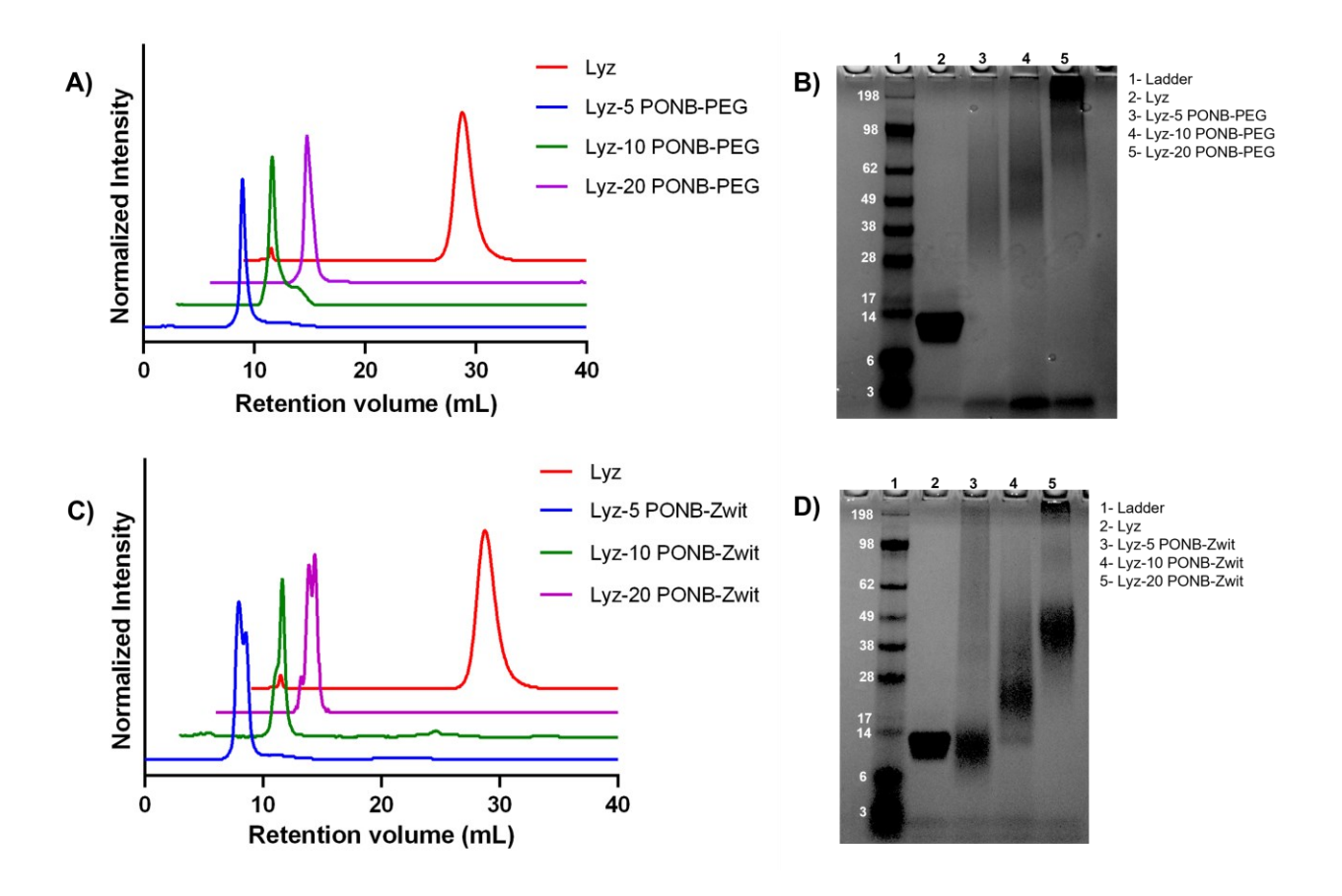


Figure 3. Characterization of grafting-to Lyz-PONB conjugates

A) FPLC traces of Lyz-PONB-PEG conjugates **B)** SDS-PAGE of Lyz-PONB-PEG conjugates **C)** FPLC traces of Lyz-PONB-Zwit conjugates **D)** SDS-PAGE of Lyz-PONB-Zwit conjugates (Absorbances were detected at 280 nm and normalized. SDS-PAGE gels were stained by Coomassie blue)

The purified **Lyz-PONB** conjugates were then used to study enzymatic activity to investigate the effect of grafting-to bioconjugation of **PONB** polymers (**Figure 4**). The activities were assessed using glycol chitosan as a substrate and were compared to unmodified **Lyz**. Most conjugations resulted in slightly lower activities compared to unmodified **Lyz**, as expected, with increasing molecular weights of **PONB** block copolymers leading to decreasing activities of the conjugates. Reduced bioactivities

observed in conjugates may arise from a combination of factors, including steric hindrance caused by polymers impeding access to the active site, alterations in protein conformation or denaturation during conjugation, and non-specific or random conjugation rather than site-specific conjugation.^{46,79,80} The Lyz-PONB-PEG conjugates retained up to 84.5% of enzymatic activity while Lyz-PONB-Zwit retained up to 97.8% of their bioactivity compared to Lyz and declined as a function of increased polymer molecular weight. The observed decrease in retained activity with increasing polymer molecular weight can be attributed to an increase in steric hindrance. Additionally, it has been observed that zwitterionic polymers can enhance the binding affinity of substrates to enzymes.^{53–55,57} Although Lyz-PONB-Zwit conjugates exhibited lower activity compared to unmodified Lyz, the extent of activity loss was mitigated. Hence, the higher retained activity observed in Lyz-PONB-Zwit conjugates, as compared to Lyz-PONB-PEG conjugates, may be attributed to this improved affinity.

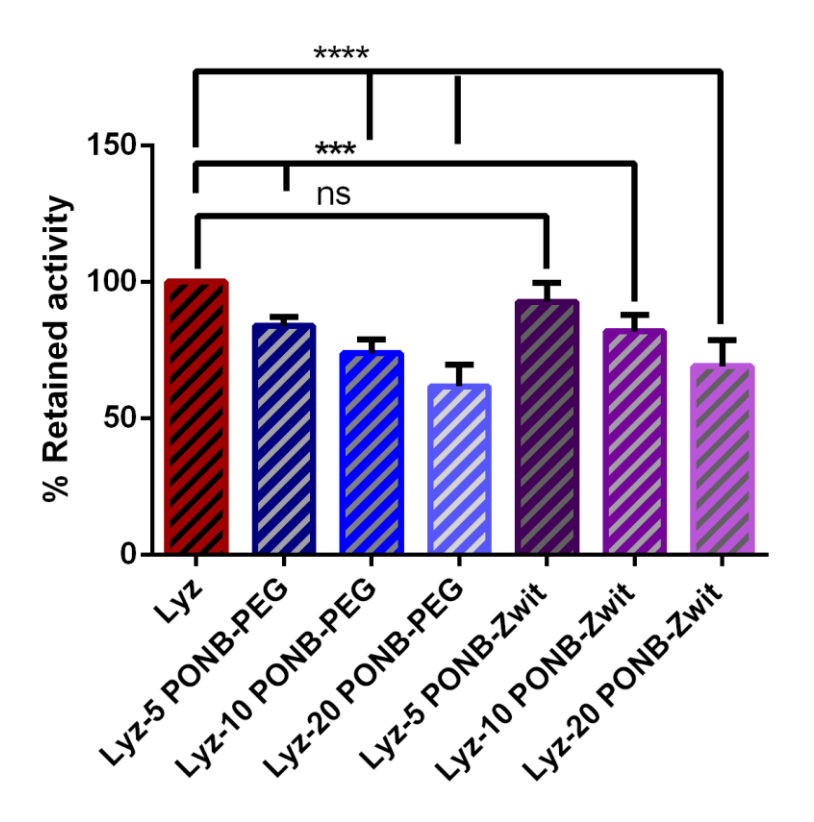


Figure 4. Enzymatic activity of grafting-to Lyz-PONB conjugates.

Glycol chitosan was used as the assay substrate and absorbance was measured at 420 nm. The absorbance of all the Lyz-PONB conjugates were normalized against Lyz. Data represented are mean ± standard deviation (N=3). The significance measurements were determined by a 2-way ANOVA test relative to the positive control. The significance markers indicate either no significant differences (n.s.), ***p=0.0002 and ****p<0.0001.

Synthesis of grafting-to uricase conjugates, UO-PONB. UO was obtained from *Bacillus fastidiosus* (~148 kDa) and is a homotetrameric enzyme in its active form. The mass analysis of the enzyme shows a molecular weight of ~37 kDa for the monomeric units (**Figure S12**). Each monomer has ~16 lysine residues, therefore a total of 64 lysine residues.⁸¹ **PONB-PEG** and **PONB-Zwit** co-polymers were covalently conjugated to the

lysine residues of the enzyme. ~20 equivalents of polymer per lysine residue was used for the conjugation and was carried out in the presence of excess uric acid (UA) in the reaction mixture. UA is the substrate for **UO** and was added to the conjugation reaction mixture to protect the enzyme active site thereby preventing substantial loss of bioactivity.⁸² The active site protection of **UO** by UA has been previously reported by Veronese and coworkers.^{82,83} The crude conjugates were purified by FPLC and showed elution volumes between 7-10 mL and 12 mL corresponding to the pure conjugates and unreacted **UO**, respectively. The purity of the **UO-PONB** conjugates was further verified by FPLC and SDS-PAGE.

SDS-PAGE was performed in denaturing conditions and gels of all UO-PONB conjugates were stained by Coomassie blue (Figure 5D-E). Analysis of protein bands of UO (Lane 2) reveal both monomer and dimer while UO-PONB conjugates (Lane 3-5) exhibited lower mobilities indicative of higher molecular weights after successful bioconjugation. UO-PONB-PEG conjugates were additionally treated with iodine to visualize PEG containing bioconjugates (Figure S13). This revealed an increase in intensity of the conjugate bands with an increase in the molecular weight of PONB-PEG conjugated to UO. The increase confirms the presence of increasing PEG composition in the conjugates. SDS-PAGE analysis of UO-PONB-Zwit (Lane 3-5) also revealed broad bands with a significantly retarded mobility that was dependent on the molecular weight of the polymer conjugates. Subsequent FPLC characterization of the purified conjugates indicated the presence of peaks from 7-10 mL corresponding to pure UO-PONB conjugates (Figure 5B-C). All the FPLC traces were unimodal except for UO-20 PONB-Zwit conjugate which showed a broader multimodal distribution. The multimodal

distribution of **UO-20 PONB-Zwit** was also observed as a broad streak in the SDS-PAGE of the conjugate (**Figure 5E**, Lane 5).

Subsequent characterizations of the conjugates were aimed towards studying the activities and immune recognition of **UO-PONB** conjugates to compare with unmodified UO and a PEGylated counterpart of UO, **UO-PEG** (Figure S14 and S15). Hence, we utilized N-hydroxylsuccinimide functionalized methoxy polyethylene glycol-10 kDa (mPEG-NHS 10 K) targeting lysine residues to synthesize a grafting-to **UO-PEG** for comparative studies. Degree of modification of UO obtained from TNBS assay were similar within conjugates derived from same type **PONB** polymers and did not decrease with increasing polymer molecular weight (**Table S2**).

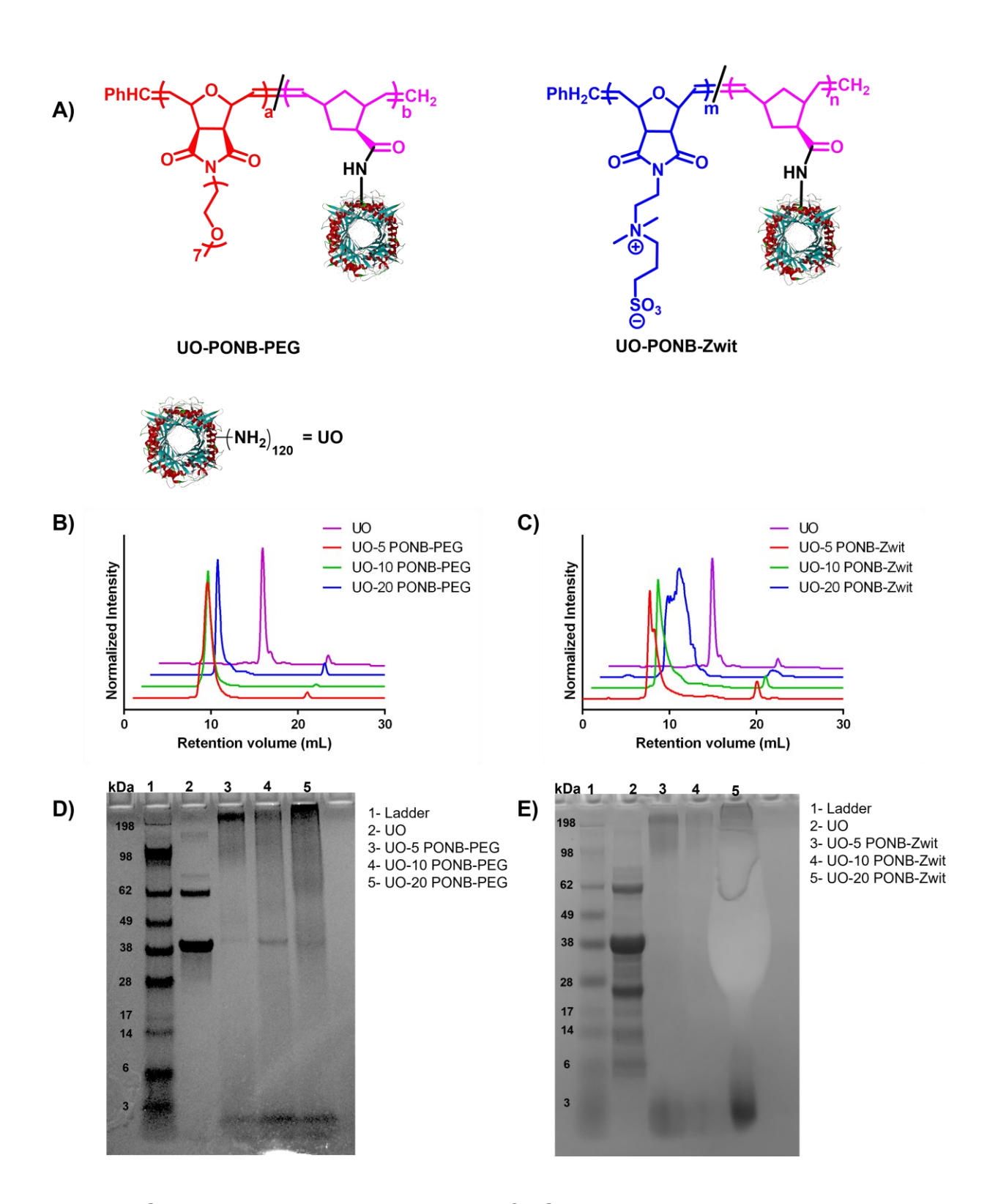


Figure 5. Synthesis and characterization of UO conjugates.

A) Grafting-to UO-PONB conjugate structures **B)** FPLC traces of grafting-to **UO-PONB-PEG** conjugates **C)** FPLC traces of grafting-to **UO-PONB-Zwit** conjugates (D) SDS-PAGE of grafting-to **UO-PONB-PEG** conjugates (E) SDS-PAGE of grafting-to **UO-PONB-Zwit** conjugates.

Bioactivity of UO conjugates. The activity of UO conjugates was determined fluorometrically, using Amplex red reagent. During the assay, the substrate uric acid is converted to allantoin, producing H₂O₂ as a byproduct. The H₂O₂ then reacts stoichiometrically with Amplex red in the presence of horseradish peroxidase (HRP), to produce the red-fluorescent product resorufin. The syntheses of UO-PONB conjugates were conducted both in the presence and absence of the UO enzyme substrate, uric acid (Figure 6). Interestingly, all UO-PONB conjugates obtained from synthesis in the absence of uric acid displayed poor activities, < 6% compared to unmodified UO, while **UO-PEG** retained activity of 28%. A substantial increase in the activities of the **UO-PONB** and UO-PEG conjugates was achieved when the conjugation was instead carried out in the presence of an excess of uric acid. The activity of **UO-PONB** and **UO-PEG** conjugates increased to 33-65% and 60%, respectively, when compared to unmodified UO. Similar observations regarding the addition of uric acid in the conjugation mixture have been reported by Veronese and co-workers demonstrating an increase in activity retention of UO after bioconjugation.^{83,84} The retention of enzymatic activity can be attributed to the 'active site protection' function of uric acid, reducing the chance of lysine modifications near the active site. This phenomenon is well reported in several enzyme systems.85-87

In addition, the kinetic parameters such as K_m (Michaelis-Menten constant), V_{max} (maximum reaction velocity) and k_{cat} (catalytic rate) of **UO** and UO conjugates were

calculated from Lineweaver-Burk plots (**Table S2**). UA in 0.5 M borate buffer (8.5 pH) at different concentrations (10-50 μ M) were catalyzed in the presence of equal amounts of **UO** or UO conjugates and the decrease in UA was detected spectrophotometrically at 292 nm. K_m represents the binding affinity of the enzyme and indicates how fast V_{max} can be achieved. K_m increased for all the conjugates compared to **UO** suggesting lower binding affinity of UO to the substrate after conjugation. Conjugation also resulted in lower V_{max} and lower k_{cat} compared to **UO**. No specific trend was observed in the kinetic constants as a function of polymer molecular weight.

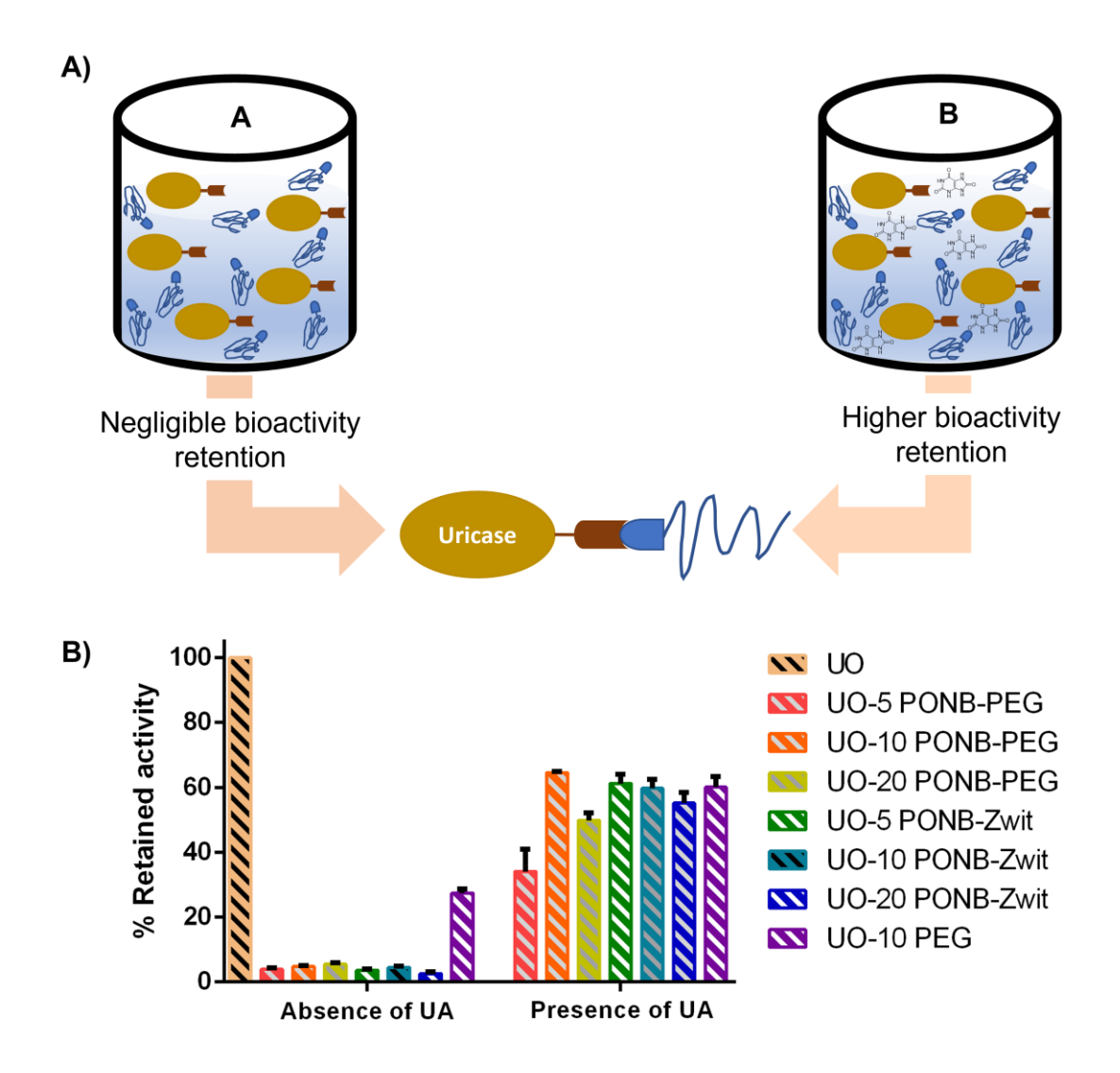


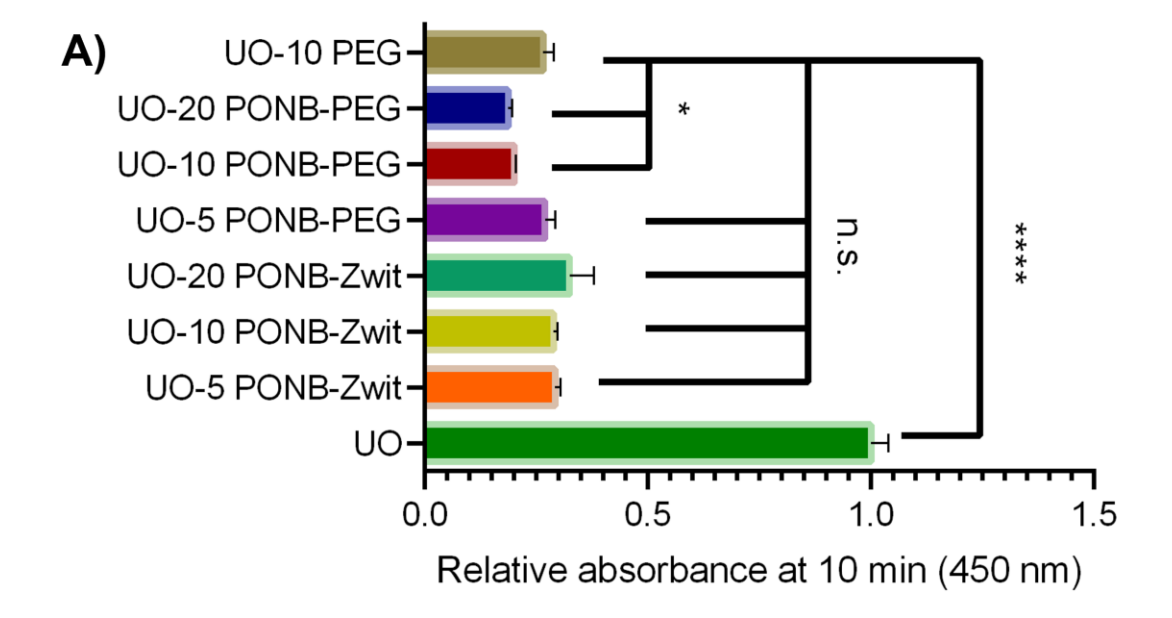
Figure 6. Retained bioactivity of UO-PONB and UO-PEG conjugates.

A) Schematic representation of conjugation. A and B represents conjugation in the absence and presence of uric acid, respectively **B)** Retained activity of UO conjugates in the presence and absence of uric acid. The activity was determined by the fluorometric detection of resorufin, an oxidation product when Amplex red reacts with H_2O_2 in the presence of HRP.

Immunogenicity of UO conjugates and anti-PEG antibody recognition. Previous studies from our lab have demonstrated reduction in protein immunogenicity as a result of polymer conjugations. 6,58-60,88 The polymers conjugated to the proteins form a protective corona making the protein antigenic sites inaccessible to antibodies and prevent aggregation and uptake of the proteins into macrophages and other clearance cells.89 To quantify the reduction in immunogenicity of UO after bioconjugation, ELISA was performed utilizing anti-UO antibodies on each UO conjugate (Figure 7A). The absorbances were normalized to unmodified UO and showed significant reduction in immune recognition for all conjugates. Greater than a 3-fold reduction in recognition of UO was observed in all the UO-PONB conjugates and all were as, or more, effective compared to **UO-PEG**. **PONB-PEG** polymers showed slightly better efficacy in reducing immune recognition compared to PONB-Zwit. UO-PONB-PEG conjugates indicated recognition as low as 18% percent compared to native UO, with the efficacy of immunoshielding increasing with increasing molecular weight of PONB-PEG while the immune recognition of **UO-PONB-Zwit** conjugates decreased to 29-32%.

Furthermore, the recognition of **UO-PONB** conjugates by anti-PEG antibodies was investigated to study the effectiveness of PONB polymers to evade immune recognition by pre-existing anti-PEG antibodies (**Figure 7B**). The anti-PEG antibodies utilized in our study exhibit specific affinity towards the ethylene oxide repeat units present in PEG. The highest recognition signal was observed with the **UO-PEG** conjugate which was used to normalize signals of all the other samples. All **UO-PONB-PEG** conjugates elicited high anti-PEG immune recognitions, nearly reaching the control signals of **UO-PEG**. **UO-20 PONB-PEG** conjugate had significant PEG specific immune recognition comparable to

UO-PEG, and the remaining **UO-PONB-PEG** conjugates showed immune recognitions as high as 60-73%. Higher anti-PEG recognition was observed with **UO-10 PONB-PEG** compared to **UO-5 PONB-PEG** due to higher PEG composition. This contrasts with previous studies, whereby short PEG-containing brush polymers showed minimal recognition and highlights the need for alternatives that have no PEG functionality in the polymer. In contrast, all **UO-PONB-Zwit** conjugates showed <10% immune recognition by anti-PEG antibodies. This is a result that is clearly expected but could have implications for those exhibiting PEG-allergies or those that have pre-existing PEG-specific antibodies.



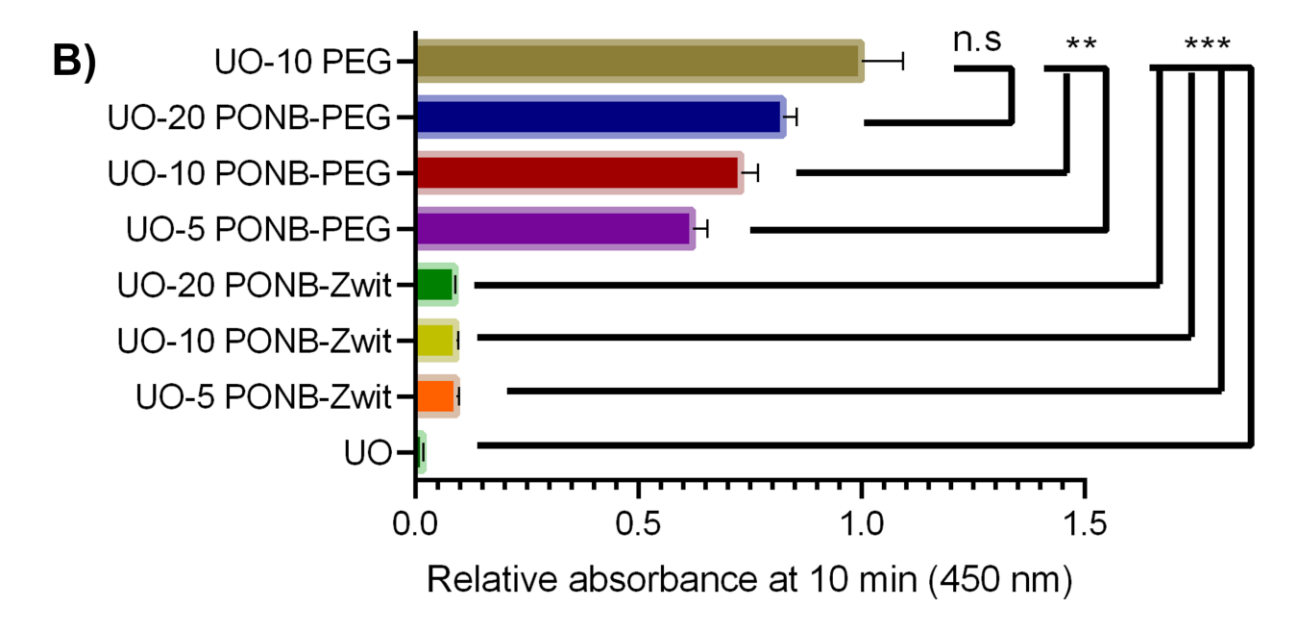


Figure 7. ELISA to study immune recognition of UO conjugates.

A) Immune recognition by anti-UO antibodies **B)** Immune recognition by anti-PEG antibodies. The relative absorbance at 450 nm after a 10-minute reaction of HRP from a two-step ELISA for (a) uricase detection and (b) PEG detection. The signal intensity was

normalized to (a) UO and (b) UO-10 PEG. Data represented are mean ± standard deviation (N=3). Significance was determined using Welch's t-test for each sample in comparison with (a) UO and (b) UO-PEG.

CONCLUSION

Investigating polymeric alternatives to PEGylation in protein-polymer conjugation has been of interest for several decades. Recent studies from our lab demonstrated the effectiveness of PNB based polymers in reducing immune recognition of protein-polymer conjugates. ^{58–60} In our current study, protein bioconjugates using **PONBs** of both a model protein, Lyz, and the therapeutically relevant UO enzyme were successfully synthesized. The conjugates retained significant bioactivity of 62-94% for Lyz-PONB and 33-65% for UO-PONB. Grafting-to bioconjugation of **PONB** based block co-polymers, **PONB-PEG** and **PONB-Zwit**, to UO led to greater than 3-fold reduction in immunogenicity. UO conjugates of **PONB-Zwit** block co-polymers demonstrated promise as a potential alternative for PEG polymer in bioconjugation because they retain high activity, minimize protein recognition, and avoid PEG-specific antibodies that may pre-exist in the population.

MATERIALS AND REAGENTS

oNB-PEG, oNB-Zwit and NB-NHS were synthesized following previously published procedures.^{67,90,91} Lysozyme, 2,4,6-Trinitrobenzene Sulfonic Acid (TNBSA or TNBS), Invitrogen™ NuPAGE™ MES SDS Running Buffer (20X), 2,2,2-Trifluoroethanol, Invitrogen™ SeeBlue™ Plus2 Pre-stained Protein Standard, GelCode™ Blue Safe Protein Stain were purchased from Thermo Fisher Scientific. mPAGE™ 4-12% Bis-Tris

Precast Gel, 10x8 cm, 12-well was purchased from Millipore Sigma. Uricase enzyme from Bacillus fastidiosus, mPEG-NHS-10 K, G2 initiator, ethyl vinyl ether and uric acid were purchased from Sigma Aldrich. Methoxypolyethylene glycol 350 (mPEG-350), ptoluenesulfonyl chloride, exo-5-Norbornenecarboxylic acid, maleimide, furan, N-Hydroxysuccinimide 1-(3-Dimethylaminopropyl)-3-ethylcarbodiimide (NHS), hydrochloride (EDC.HCI), pyridine, N,N-dimethylethylenediamine and 1,3propanesultone were purchased from TCI Chemicals. Anti-uricase antibody was purchased by Rockland, anti-PEG antibody was purchased from Sigma, and the secondary antibodies were purchased from Invitrogen.

INSTRUMENTATION

Nuclear Magnetic Resonance (NMR) spectra were obtained using a 300 MHz Bruker AVA. All NMRs were calibrated against corresponding solvent peaks. PONB-PEG NMR was obtained in CDCl₃ while PONB-Zwit NMR was obtained in D₂O. Shimadzu Prominence GPC instrument, used for the analysis of PONB-PEG polymers was equipped with a Shimadzu RID10A differential refractometer detector. The GPC system employed two Phenomenex 10E3A size exclusion columns in sequence, which were maintained at a temperature of 30 °C. Anhydrous THF was used as the mobile phase for GPC analysis, with a flow rate of 1.0 mL/min. All polymer samples were filtered using 0.22-micron PTFE syringe filters before injection. The GPC instrument used for the characterization of PONB-Zwit polymers was equipped with Waters Ultrahydrogel SEC Columns. 70/30 (v/v) ratio of aqueous phosphate buffer to methanol was used as the mobile phase with a flow rate of 1.0 mL/min. Polymer solutions were dissolved by overnight stirring and filtered using 0.22-micron PTFE syringe filters to avoid aggregates.

Matrix-assisted laser desorption/ionization-time of flight mass spectrometry (MALDI-TOF MS) was performed on Bruker Autoflex Max. Agilent 6230 LC-ESI-TOFMS was used to obtain molecular weight data of UO.

Fast protein liquid chromatography (FPLC) was performed using a GE Healthcare AKTA FPLC 900 chromatography system equipped with a Superdex 75 10/300 or Superdex 200 Increase 10/300 size exclusion column. Superdex 75 10/300 was used in the case of Lyz conjugates, while Superdex 200 Increase 10/300 was equipped for UO conjugates. For all FPLC experiments, the mobile phase was 1X phosphate buffer saline (PBS), (pH 7.4) at a flow rate of 0.4 mL/min at 4 °C. Sodium Dodecyl Sulfate- Polyacrylamide Gel Electrophoresis (SDS-PAGE) was performed in mPAGE™ 4-12% Bis-Tris Precast Gels, (10x8 cm, 12-well), 1X Invitrogen™ NuPAGE™ MES SDS Running Buffer was used as running buffer for the gels and every gel was run with Invitrogen™ SeeBlue™ Plus2 Prestained Protein Standard. The gels were washed (3X) before staining them with 20 mL of 1X GelCode™ Blue Safe Protein Stain and/or 1X lodine (1.9%). The gels stained by GelCode™ Blue Safe Protein Stain destained anywhere from 30 minutes – 4hours. Iodine destained much faster (less than 30 minutes). The concentration of proteins and protein conjugates were obtained from Bradford assay using BSA as standards. Microplate measurements were obtained with a Biotek Synergy HT microplate reader.

METHODS

Synthesis of PONB-PEG co-polymer. 20 mL glass scintillation vial was flame dried and purged with N_2 for 10 minutes. **oNB-PEG** (1 g, 2 mmol, 1 equivalent) was dissolved in anhydrous DCM before adding into the glass vial. **G3** initiator (5 kDa: 0.146 g, 0.2 mmol, 0.099 equivalent; 10 kDa: 0.073 g, 0.1 mmol, 0.05 equivalent; 20 kDa: 0.037 g, 0.05

mmol, 0.025 equivalents) was dissolved in anhydrous DCM and added at once. Polymerization was allowed the proceed for 15 minutes before the addition of monomer, **NB-NHS**. **NB-NHS** (5 kDa: 0.131 g, 0.8 mmol, 0.399 equivalent; 10 kDa: 0.066 g, 0.4 mmol, 0.2 equivalent; 20 kDa: 0.033 g, 0.2 mmol, 0.1 equivalent) was dissolved in DCM and added to the polymer solution. This was allowed to react for another 15 minutes. 1 mL ethyl vinyl ether (EVE) was added to the solution to terminate the polymerization and was reacted for 30 minutes. The terminated polymer solution was concentrated to 0.3 mL and was precipitated in excess pentane. The pentane was decanted, and the amber oil viscous polymer was characterized by ¹H NMR (**Figure S1-S4**), GPC (**Figure 1B**) and SDS-PAGE (**Figure S5**).

Synthesis of PONB-Zwit copolymers. 20 mL glass scintillation vial was flame dried and purged with N₂ for 10 minutes. oNB-Zwit (1 g, 2.8 mmol, 1 equivalent) was dissolved in 1:1 TFE/DCM solvent mixture. G3 initiator (5 kDa: 0.146 g, 0.2 mmol, 0.099 equivalent; 10 kDa: 0.073 g, 0.1 mmol, 0.05 equivalent; 20 kDa: 0.037 g, 0.05 mmol, 0.025 equivalents) was dissolved in DCM and added at once. The polymerization was allowed to proceed for 40 minutes before the addition of the capping agent NB-NHS ester. NB-NHS ester was dissolved in DCM and added to the polymerization solution. This was allowed to react for 20 minutes and was terminated by adding 1 mL EVE into the polymerization solution. The termination was allowed to proceed for 30 minutes. The gellike amber oil polymer was precipitated into excess THF. The precipitate was filtered through a sintered funnel and was dried in vacuum. The product was a whitish brown color powder. The polymers were characterized by ¹H NMR (Figure 2, S8 and S9) and MALDI-TOF MS (Figure S6).

Synthesis of Lysozyme-PONB-PEG (Lyz-PONB-PEG) and Lysozyme-PONB-Zwit (Lyz-PONB-Zwit) conjugates. In a 20 mL glass scintillation vial lysozyme (0.5 mg, 35 nmol, 1 equivalent) was dissolved in 0.5 mL of PBS, pH 7.4. **PONB-PEG** co-polymer (5 kDa: 13.2 mg; 10 kDa: 26.3 mg; 20 kDa: 52.5 mg; 2.6 µmol, 75 equivalent) was dissolved in 0.2 mL DMSO and **PONB-Zwit** co-polymer (5 kDa: 13.2 mg; 10 kDa: 26.3 mg; 20 kDa: 52.5 mg; 2.6 µmol, 75 equivalent) was dissolved in 0.2 mL PBS, pH 7.4 by sonication and was added slowly to the lysozyme solution. The conjugation was allowed to proceed for 4 hours, after which the solution was concentrated using a 10 kDa MWCO Amicon Ultra-4 centrifugal units to a final volume of ~300 µL. The concentrated conjugate solution was purified by FPLC. A Superdex 75 (10/300) column was used, and the sample was eluted in PBS, 7.4 buffer at flow rate of 0.4 mL/min. The pure conjugates were eluted at 7-10 mL retention volumes while unreacted lysozyme eluted at ~20 mL. The purified conjugate was concentrated by centrifuge filtration using 10 kDa MWCO Amicon ultra-4 centrifugal filter units. The concentration of the protein was determined by Bradford assay. The purified conjugates were characterized by SDS-PAGE (Figure 3B and 3D) and FPLC (Figure 3A and 3C).

Lysozyme activity assay for Lyz and Lyz-PONB conjugates. The activity of the Lyz-PONB conjugates were assayed using glycol chitosan as the substrate. First, a 0.05% (w/v) glycol chitosan was prepared in 100 mM acetate buffer, pH 5.5. Secondly, a 1.52 mM potassium ferricyanide solution was freshly prepared in 0.5 M sodium carbonate. 1 mL of the glycol chitosan solution was mixed with 100 μL of lysozyme or Lyz-PONB conjugates and incubated at 40 °C for 30 minutes. To this, a 2 mL potassium ferricyanide solution was added and immediately brought to and held at boil for 15 minutes. The

mixture was allowed to cool down. 200 µL of the samples were plated onto a 96-well plate in triplicates. The absorbance was measured at 420 nm (**Figure 4**).

Synthesis of UO-PONB-PEG and UO-PONB-Zwit conjugates. In a 20 mL glass scintillation vial Uricase enzyme (0.5 mg, 11.4 nmol, 1 equivalent) was dissolved in 0.5 mL of 0.2 M borate buffer pH 8.5. To this enzyme solution, PONB-PEG co-polymer (5 kDa: 17.2 mg; 10 kDa: 34.3 mg; 20 kDa: 68.6 mg; 3.5 µmol, 300 equivalent) dissolved in 0.2 mL DMSO and **PONB-Zwit** (5 kDa: 17.2 mg; 10 kDa: 34.3 mg; 20 kDa: 68.6 mg; 3.5 µmol, 300 equivalent) dissolved in 0.2 mL 0.2 M borate buffer pH 8.5. The final pH of the reaction solution was maintained at 8.5-9.0 by the addition of 1 N NaOH. The conjugation was allowed for 4 hours, and the solution was concentrated to a final volume of 0.25 mL by 10 kDa MWCO Amicon Ultra-4 centrifugal filter units. The concentrated conjugate was purified using the FPLC. A Superdex 75 (10/300) column was used, and the sample was eluted in PBS, 7.4 buffer at flow rate of 0.4 mL/min. The pure conjugates eluted at 7-10 mL while the unreacted uricase peak eluted at 12 mL. The purified conjugate was concentrated by centrifuge filtration using 10 kDa MWCO Amicon Ultra-4 centrifugal filter units. The concentration of the purified conjugates was determined using a Bradford assay. The pure conjugates were characterized by SDS-PAGE (Figure 5 D-E) and FPLC (Figure 5 B-C).

Synthesis of UO-PEG conjugate. In a 20 mL glass scintillation vial **UO** (0.5 mg, 11.4 nmol, 1 equivalent) was dissolved in 0.5 mL of 0.2 M borate buffer pH 8.5. To this **UO** solution, **mPEG-NHS-10 K** (10 kDa; 43 mg, 4.3 μmol, 300 equivalents) dissolved in 0.5 mL of borate buffer was added slowly over 30 minutes. The conjugation reaction was allowed for 4 hours, and the solution was concentrated to a final volume of 0.25 mL by

centrifuge filtration using 10 kDa MWCO Amicon Ultra-4 centrifugal filter units. The concentrated conjugate was purified by performing FPLC. A Superdex 75 (10/300) column was used, and the sample was eluted in PBS, 7.4 buffer at flow rate of 0.4 mL/min. The pure conjugate eluted at 7-10 mL while the unreacted uricase peak eluted at 12 mL. The purified conjugate was concentrated by 10 kDa MWCO Amicon Ultra-4 centrifugal filter units. The concentration of the purified conjugates was determined using BCA protein assay. The pure conjugates were characterized by SDS-PAGE (**Figure S15**) and FPLC (**Figure S14**).

Uricase activity assay for UO and UO conjugates. The uricase activity was measured based on the fluorometric detection of resorufin, a red-fluorescent oxidation product generated when H_2O_2 reacts with Amplex Red reagent in the presence of horseradish peroxidase (HRP).

Prepare the working solution for the assay: 3.93 mL of 0.5 M Tris HCl buffer, pH 7.5, 20 μL of 100 U/mL HRP in 0.5 M Tris HCl buffer, pH 7.5, 1 mL of 5 mM UA and 50 μL of 10 mM Amplex red reagent dissolved in DMSO was mixed to prepare 5 mL of the working solution. Note: Amplex red reagent is light sensitive.

50 μL of UO, UO conjugates (5 mU/mL) and blank (0.5 M Tris HCl buffer, pH 7.5) were added to a black 96-well plate in triplicates. To these sample solutions, 50 μL of working solution was added. Fluorescence was measured after incubating at 25 °C for 30 minutes using excitation in the range of 530-560 nm and emission was detected at 590 nm. The activity of UO was considered 100% and the activities of conjugates were normalized with the activity of UO.

TNBS assay. 100 μ L of 0.2 mg/mL protein or protein conjugate solution in 0.5 M borate buffer, pH 8.5 was mixed with 50 μ L of 0.1 % (w/v) (diluted fresh from 5 % (w/v) in H2O solution using 0.5 M borate buffer, pH 8.5) in a 96-well plate. The mixture was incubated for 2 hours at 37 °C in dark. The absorbance was detected at 335 nm. The absorbance indicates free amino groups and conjugation results in lower absorbance compared to unmodified proteins. (The assay protocol generally suggests addition of 10% SDS and 1M HCl for termination, however this resulted in a cloudy solution in our case. Therefore, this step was eliminated)

Enzyme kinetics of UO and UO conjugates. The enzyme kinetics of UO and UO conjugates were studies based on oxidation of uric acid substrate. Substrate (UA) concentrations (0, 10, 20, 30, 40, 50 μM) were prepared in 0.5 M borate buffer, pH 8.5. 150 μL of each UA concentration was well mixed with 10 μL of 100 ug/mL UO or UO conjugates in a 96-well plate. Absorbance was detected at 292 nm over time (10 mins). The linear section of this plot was used to calculate the initial rate of the reaction (v). Microplate based pathlength correction was performed using the following equation,

 $Pathlength = \frac{A975 \, (well) - A900 \, (well)}{K - Factor}$, the K-Factor was considered 0.173 for aqueous buffers.

The kinetics constants were determined using a Lineweaver-Burk plot. 92

ELISA Immune assay. Uricase and uricase-polymer conjugates were coated onto each well of the Thermo Scientific NUNC 96-well plates using coating buffer (0.1 M KP buffer, pH 7.0) overnight in a shaker at 4 °C (10 μg mL⁻¹). The wells were washed three times with 200 μL of wash solution (0.05% (w/v) Tween 20 in PBS) using an accuWash (Fisher

Scientific). The wells were coated with 100 µL of 3% BSA (w/v) in 1X PBS and left to shake overnight at 4 °C. The washing protocol was repeated. Primary antibody solutions were prepared at 2.1 mg/mL with 5% BSA (w/v) in 1X PBS (for uricase detection, goatderived anti-uricase antibody from Rockland (200-101-0925, Lot 37209); for PEG detection, rat-derived anti-PEG antibody (MABS1962, clone rAGP6, Lot 3724609 from EMD Millipore Sigma). To each well, 100 µL of primary antibody solution was added and incubated at 25 °C under agitation for 1 hour. The washing protocol was repeated. Secondary antibody solutions were prepared at 0.2 µg/mL with 5% BSA (w/v) in 1X PBS (for uricase detection, donkey anti-goat IgG (H + L) horseradish peroxidase (HRP) conjugates from Invitrogen, (A15999, Lot 967125); for PEG detection, goat anti-rat IgM HRP from Invitrogen (31476, Lot XF3603641). To each well, 100 µL of secondary antibody solution was added and incubated at 25 °C under agitation for 1 hour. The washing protocol was repeated. For detection, 100 µL of room temperature 1-Step Ultra TMB-ELISA Substrate Solution (Thermo Scientific, 34028) was added to the wells. After 2 minutes, the reaction was quenched with 100 mL of 2N H₂SO₄. The absorbance of the solutions at 650 nm was measured using a plate reader (Tecan Infinite M Plex). Significance measurements were performed in Prism 9 (GraphPad) using Welch's t-test.

ACKNOWLEDGEMENTS

This work was sponsored primarily by the UC San Diego Materials Research Science and Engineering Center (UCSD MRSEC), supported by the National Science Foundation (Grant DMR-2011924) and in part by the NSF chemistry program (CHE 180803). The National Institute of Food and Agriculture provided additional support (NIFA-2022-67012-36698). The authors would like to thank Dr. Derek C Church, Dr. Debika Datta and Dr.

Han Sol Kim for valuable discussions. The authors would like to also thank the UCSD

Skaggs School of Pharmacy and Pharmaceutical Sciences NMR Facility and Dr. Brendan

M. Duggan for NMR support.

NOTES

Authors declare no conflict of interest.

AUTHOR INFORMATION

Corresponding author

Jonathan K. Pokorski- Department of NanoEngineering, Center for Nano-

ImmunoEngineering, Institute for Materials Discovery and Design, University of

California San Diego, La Jolla CA 92039, USA.

Email- jpokorski@ucsd.edu

Authors

Elizabathe Davis- Department of NanoEngineering, University of California San Diego,

La Jolla CA 92039, USA.

ORCID iD: 0000-0002-6807-2874

Adam A. Caparco- Department of NanoEngineering, University of California San

Diego, La Jolla CA 92039, USA.

ORCID iD: 0000-0002-8545-8349

Nicole F. Steinmetz- Department of NanoEngineering, Center for Nano-ImmunoEngineering, Institute for Materials Discovery and Design, Department of Bioengineering, Department of Radiology, Moores Cancer Center, University of California San Diego, La Jolla CA 92039, USA.

REFERENCES

- (1) Abuchowski, A.; van Es, T.; Palczuk, N. C.; Davis, F. F. Alteration of Immunological Properties of Bovine Serum Albumin by Covalent Attachment of Polyethylene Glycol. *Journal of Biological Chemistry* 1977, 252 (11), 3578–3581. https://doi.org/10.1016/S0021-9258(17)40291-2.
- (2) Abuchowski, A.; McCoy, J. R.; Palczuk, N. C.; van Es, T.; Davis, F. F. Effect of Covalent Attachment of Polyethylene Glycol on Immunogenicity and Circulating Life of Bovine Liver Catalase. *Journal of Biological Chemistry* **1977**, 252 (11), 3582–3586. https://doi.org/10.1016/S0021-9258(17)40292-4.
- (3) Inada, Y.; Matsuswma, A.; Kodera, Y.; Nishimura, H. Review: Polyethylene Glycol(PEG)-Protein Conjugates: Application to Biomedical and Biotechnological Processes. *Journal of Bioactive and Compatible Polymers* 1990, 5 (3), 343–364. https://doi.org/10.1177/088391159000500309.
- (4) Nucci, M. L.; Shorr, R.; Abuchowski, A. The Therapeutic Value of Poly(Ethylene Glycol)-Modified Proteins. *Advanced Drug Delivery Reviews* 1991, 6 (2), 133–151. https://doi.org/10.1016/0169-409X(91)90037-D.

- (5) Alconcel, S. N. S.; Baas, A. S.; Maynard, H. D. FDA-Approved Poly(Ethylene Glycol)–Protein Conjugate Drugs. *Polym. Chem.* 2011, 2 (7), 1442–1448. https://doi.org/10.1039/C1PY00034A.
- (6) Duncan, R. The Dawning Era of Polymer Therapeutics. *Nat Rev Drug Discov* 2003, 2 (5), 347–360. https://doi.org/10.1038/nrd1088.
- (7) Harris, J. M.; Chess, R. B. Effect of Pegylation on Pharmaceuticals. *Nat Rev Drug Discov* **2003**, *2* (3), 214–221. https://doi.org/10.1038/nrd1033.
- (8) Harris, J. M.; Martin, N. E.; Modi, M. Pegylation. *Clin Pharmacokinet* **2001**, *40* (7), 539–551. https://doi.org/10.2165/00003088-200140070-00005.
- (9) Hong, L.; Wang, Z.; Wei, X.; Shi, J.; Li, C. Antibodies against Polyethylene Glycol in Human Blood: A Literature Review. *Journal of Pharmacological and Toxicological Methods* 2020, 102, 106678.
 https://doi.org/10.1016/j.vascn.2020.106678.
- (10) Shimizu, T.; Mima, Y.; Hashimoto, Y.; Ukawa, M.; Ando, H.; Kiwada, H.; Ishida, T. Anti-PEG IgM and Complement System Are Required for the Association of Second Doses of PEGylated Liposomes with Splenic Marginal Zone B Cells. Immunobiology 2015, 220 (10), 1151–1160. https://doi.org/10.1016/j.imbio.2015.06.005.
- (11) Yang, Q.; Lai, S. K. Anti-PEG Immunity: Emergence, Characteristics, and Unaddressed Questions. WIREs Nanomedicine and Nanobiotechnology 2015, 7 (5), 655–677. https://doi.org/10.1002/wnan.1339.
- (12) Garay, R. P.; El-Gewely, R.; Armstrong, J. K.; Garratty, G.; Richette, P. Antibodies against Polyethylene Glycol in Healthy Subjects and in Patients Treated with PEG-

- Conjugated Agents. *Expert Opinion on Drug Delivery* **2012**, 9 (11), 1319–1323. https://doi.org/10.1517/17425247.2012.720969.
- (13) P. Garay, R.; P. Labaune, J. Immunogenicity of Polyethylene Glycol (PEG). *The Open Conference Proceedings Journal* **2011**, *2* (1).
- (14) Richter, A. W.; Åkerblom, E. Polyethylene Glycol Reactive Antibodies in Man: Titer Distribution in Allergic Patients Treated with Monomethoxy Polyethylene Glycol Modified Allergens or Placebo, and in Healthy Blood Donors. *IAA* 1984, 74 (1), 36–39. https://doi.org/10.1159/000233512.
- (15) Chen, B.-M.; Su, Y.-C.; Chang, C.-J.; Burnouf, P.-A.; Chuang, K.-H.; Chen, C.-H.; Cheng, T.-L.; Chen, Y.-T.; Wu, J.-Y.; Roffler, S. R. Measurement of Pre-Existing IgG and IgM Antibodies against Polyethylene Glycol in Healthy Individuals. *Anal. Chem.* 2016, 88 (21), 10661–10666.
 https://doi.org/10.1021/acs.analchem.6b03109.
- (16) Kozma, G. T.; Shimizu, T.; Ishida, T.; Szebeni, J. Anti-PEG Antibodies: Properties, Formation, Testing and Role in Adverse Immune Reactions to PEGylated Nano-Biopharmaceuticals. *Advanced Drug Delivery Reviews* 2020, 154–155, 163–175. https://doi.org/10.1016/j.addr.2020.07.024.
- (17) Abu Lila, A. S.; Kiwada, H.; Ishida, T. The Accelerated Blood Clearance (ABC)

 Phenomenon: Clinical Challenge and Approaches to Manage. *Journal of Controlled Release* 2013, 172 (1), 38–47. https://doi.org/10.1016/j.jconrel.2013.07.026.
- (18) Povsic, T. J.; Lawrence, M. G.; Lincoff, A. M.; Mehran, R.; Rusconi, C. P.;

 Zelenkofske, S. L.; Huang, Z.; Sailstad, J.; Armstrong, P. W.; Steg, P. G.; Bode, C.;

 Becker, R. C.; Alexander, J. H.; Adkinson, N. F.; Levinson, A. I. Pre-Existing Anti-

- PEG Antibodies Are Associated with Severe Immediate Allergic Reactions to Pegnivacogin, a PEGylated Aptamer. *Journal of Allergy and Clinical Immunology* **2016**, *138* (6), 1712–1715. https://doi.org/10.1016/j.jaci.2016.04.058.
- (19) Elsadek, N. E.; Abu Lila, A. S.; Ishida, T. 5 Immunological Responses to PEGylated Proteins: Anti-PEG Antibodies. In *Polymer-Protein Conjugates*; Pasut, G., Zalipsky, S., Eds.; Elsevier, 2020; pp 103–123. https://doi.org/10.1016/B978-0-444-64081-9.00005-X.
- (20) Eckardt, K.-U. The Safety and Efficacy of Peginesatide in Patients with CKD.
 Nature Reviews Nephrology 2013, 9 (4), 192–193.
 https://doi.org/10.1038/nrneph.2013.42.
- (21) Schlesinger, N.; Yasothan, U.; Kirkpatrick, P. Pegloticase. *Nat Rev Drug Discov* **2011**, *10* (1), 17–18. https://doi.org/10.1038/nrd3349.
- (22) Schlesinger, N.; Lipsky, P. E. Pegloticase Treatment of Chronic Refractory Gout:

 Update on Efficacy and Safety. *Seminars in Arthritis and Rheumatism* **2020**, *50* (3, Supplement), S31–S38. https://doi.org/10.1016/j.semarthrit.2020.04.011.
- (23) Hoang Thi, T. T.; Pilkington, E. H.; Nguyen, D. H.; Lee, J. S.; Park, K. D.; Truong, N. P. The Importance of Poly(Ethylene Glycol) Alternatives for Overcoming PEG Immunogenicity in Drug Delivery and Bioconjugation. *Polymers* 2020, 12 (2), 298. https://doi.org/10.3390/polym12020298.
- (24) Qi, Y.; Chilkoti, A. Protein–Polymer Conjugation Moving beyond PEGylation.
 Current Opinion in Chemical Biology 2015, 28, 181–193.
 https://doi.org/10.1016/j.cbpa.2015.08.009.

- (25) Pelegri-O'Day, E. M.; Lin, E.-W.; Maynard, H. D. Therapeutic Protein–Polymer Conjugates: Advancing Beyond PEGylation. *J. Am. Chem. Soc.* **2014**, *136* (41), 14323–14332. https://doi.org/10.1021/ja504390x.
- (26) Ashford, M. B.; England, R. M.; Akhtar, N. Highway to Success—Developing Advanced Polymer Therapeutics. *Advanced Therapeutics* 2021, 4 (5), 2000285. https://doi.org/10.1002/adtp.202000285.
- (27) Barz, M.; Luxenhofer, R.; Zentel, R.; J. Vicent, M. Overcoming the PEG-Addiction: Well-Defined Alternatives to PEG, from Structure–Property Relationships to Better Defined Therapeutics. *Polymer Chemistry* 2011, 2 (9), 1900–1918. https://doi.org/10.1039/C0PY00406E.
- (28) Knop, K.; Hoogenboom, R.; Fischer, D.; Schubert, U. S. Poly(Ethylene Glycol) in Drug Delivery: Pros and Cons as Well as Potential Alternatives. *Angewandte* Chemie International Edition 2010, 49 (36), 6288–6308. https://doi.org/10.1002/anie.200902672.
- (29) Pasut, G.; Zalipsky, S. *Polymer-Protein Conjugates: From Pegylation and Beyond*; Elsevier, 2019.
- (30) Matyjaszewski, K. Atom Transfer Radical Polymerization (ATRP): Current Status and Future Perspectives. *Macromolecules* 2012, 45 (10), 4015–4039. https://doi.org/10.1021/ma3001719.
- (31) Moad, G.; Rizzardo, E.; Thang, S. H.; Moad, G.; Rizzardo, E.; Thang, S. H. Living Radical Polymerization by the RAFT Process. *Aust. J. Chem.* **2005**, *58* (6), 379–410. https://doi.org/10.1071/CH05072.

- (32) Hawker, C. J.; Bosman, A. W.; Harth, E. New Polymer Synthesis by Nitroxide Mediated Living Radical Polymerizations. *Chem. Rev.* 2001, 101 (12), 3661–3688. https://doi.org/10.1021/cr990119u.
- (33) Bielawski, C. W.; Grubbs, R. H. Living Ring-Opening Metathesis Polymerization.
 Progress in Polymer Science 2007, 32 (1), 1–29.
 https://doi.org/10.1016/j.progpolymsci.2006.08.006.
- (34) Boyer, C.; Bulmus, V.; Davis, T. P.; Ladmiral, V.; Liu, J.; Perrier, S. Bioapplications of RAFT Polymerization. *Chem. Rev.* **2009**, *109* (11), 5402–5436. https://doi.org/10.1021/cr9001403.
- (35) Gregory, A.; Stenzel, M. H. Complex Polymer Architectures via RAFT Polymerization: From Fundamental Process to Extending the Scope Using Click Chemistry and Nature's Building Blocks. *Progress in Polymer Science* 2012, 37 (1), 38–105. https://doi.org/10.1016/j.progpolymsci.2011.08.004.
- (36) Blosch, S. E.; Scannelli, S. J.; Alaboalirat, M.; Matson, J. B. Complex Polymer Architectures Using Ring-Opening Metathesis Polymerization: Synthesis, Applications, and Practical Considerations. *Macromolecules* 2022, 55 (11), 4200–4227. https://doi.org/10.1021/acs.macromol.2c00338.
- (37) Nicolas, J.; Guillaneuf, Y.; Lefay, C.; Bertin, D.; Gigmes, D.; Charleux, B. Nitroxide-Mediated Polymerization. *Progress in Polymer Science* **2013**, 38 (1), 63–235. https://doi.org/10.1016/j.progpolymsci.2012.06.002.
- (38) Ko, J. H.; Maynard, H. D. A Guide to Maximizing the Therapeutic Potential of Protein–Polymer Conjugates by Rational Design. *Chem. Soc. Rev.* **2018**, *47* (24), 8998–9014. https://doi.org/10.1039/C8CS00606G.

- (39) Zhang, P.; Sun, F.; Liu, S.; Jiang, S. Anti-PEG Antibodies in the Clinic: Current Issues and beyond PEGylation. *Journal of Controlled Release* **2016**, *244*, 184–193. https://doi.org/10.1016/j.jconrel.2016.06.040.
- (40) Liu, X.; Sun, M.; Sun, J.; Hu, J.; Wang, Z.; Guo, J.; Gao, W. Polymerization Induced Self-Assembly of a Site-Specific Interferon α-Block Copolymer Conjugate into Micelles with Remarkably Enhanced Pharmacology. *J. Am. Chem. Soc.* 2018, 140 (33), 10435–10438. https://doi.org/10.1021/jacs.8b06013.
- (41) Weinhart, M.; Grunwald, I.; Wyszogrodzka, M.; Gaetjen, L.; Hartwig, A.; Haag, R. Linear Poly(Methyl Glycerol) and Linear Polyglycerol as Potent Protein and Cell Resistant Alternatives to Poly(Ethylene Glycol). *Chemistry An Asian Journal* 2010, 5 (9), 1992–2000. https://doi.org/10.1002/asia.201000127.
- (42) Zaghmi, A.; Greschner, A. A.; Gauthier, M. A. 17 In Vivo Properties of Therapeutic Bioconjugates Composed of Proteins and Architecturally/Functionally Complex Polymers. In *Polymer-Protein Conjugates*; Pasut, G., Zalipsky, S., Eds.; Elsevier, 2020; pp 389–406. https://doi.org/10.1016/B978-0-444-64081-9.00017-6.
- (43) Fu, C.; Demir, B.; Alcantara, S.; Kumar, V.; Han, F.; Kelly, H. G.; Tan, X.; Yu, Y.; Xu, W.; Zhao, J.; Zhang, C.; Peng, H.; Boyer, C.; Woodruff, T. M.; Kent, S. J.; Searles, D. J.; Whittaker, A. K. Low-Fouling Fluoropolymers for Bioconjugation and In Vivo Tracking. *Angewandte Chemie* 2020, *132* (12), 4759–4765. https://doi.org/10.1002/ange.201914119.
- (44) Qiao, R.; Fu, C.; Li, Y.; Qi, X.; Ni, D.; Nandakumar, A.; Siddiqui, G.; Wang, H.; Zhang, Z.; Wu, T.; Zhong, J.; Tang, S.-Y.; Pan, S.; Zhang, C.; Whittaker, M. R.; Engle, J. W.; Creek, D. J.; Caruso, F.; Ke, P. C.; Cai, W.; Whittaker, A. K.; Davis, T.

- P. Sulfoxide-Containing Polymer-Coated Nanoparticles Demonstrate Minimal Protein Fouling and Improved Blood Circulation. *Advanced Science* **2020**, 7 (13), 2000406. https://doi.org/10.1002/advs.202000406.
- (45) Yu, Y.; Xu, W.; Huang, X.; Xu, X.; Qiao, R.; Li, Y.; Han, F.; Peng, H.; Davis, T. P.; Fu, C.; Whittaker, A. K. Proteins Conjugated with Sulfoxide-Containing Polymers Show Reduced Macrophage Cellular Uptake and Improved Pharmacokinetics.
 ACS Macro Lett. 2020, 9 (6), 799–805.
 https://doi.org/10.1021/acsmacrolett.0c00291.
- (46) Morgenstern, J.; Gil Alvaradejo, G.; Bluthardt, N.; Beloqui, A.; Delaittre, G.; Hubbuch, J. Impact of Polymer Bioconjugation on Protein Stability and Activity Investigated with Discrete Conjugates: Alternatives to PEGylation. Biomacromolecules 2018, 19 (11), 4250–4262. https://doi.org/10.1021/acs.biomac.8b01020.
- (47) Gao, W.; Liu, W.; Mackay, J. A.; Zalutsky, M. R.; Toone, E. J.; Chilkoti, A. In Situ Growth of a Stoichiometric PEG-like Conjugate at a Protein's N-Terminus with Significantly Improved Pharmacokinetics. *Proceedings of the National Academy of Sciences* 2009, 106 (36), 15231–15236. https://doi.org/10.1073/pnas.0904378106.
- (48) Ozer, I.; Kelly, G.; Gu, R.; Li, X.; Zakharov, N.; Sirohi, P.; Nair, S. K.; Collier, J. H.; Hershfield, M. S.; Hucknall, A. M.; Chilkoti, A. Polyethylene Glycol-Like Brush Polymer Conjugate of a Protein Drug Does Not Induce an Antipolymer Immune Response and Has Enhanced Pharmacokinetics than Its Polyethylene Glycol Counterpart. *Advanced Science* 2022, *9* (11), 2103672. https://doi.org/10.1002/advs.202103672.

- (49) Qi, Y.; Simakova, A.; Ganson, N. J.; Li, X.; Luginbuhl, K. M.; Ozer, I.; Liu, W.; Hershfield, M. S.; Matyjaszewski, K.; Chilkoti, A. A Brush-Polymer/Exendin-4 Conjugate Reduces Blood Glucose Levels for up to Five Days and Eliminates Poly(Ethylene Glycol) Antigenicity. *Nature Biomedical Engineering* 2016, 1 (1), 1– 12. https://doi.org/10.1038/s41551-016-0002.
- (50) Heredia, K. L.; Tolstyka, Z. P.; Maynard, H. D. Aminooxy End-Functionalized Polymers Synthesized by ATRP for Chemoselective Conjugation to Proteins. *Macromolecules* 2007, 40 (14), 4772–4779. https://doi.org/10.1021/ma070432v.
- (51) Magnusson, J. P.; Bersani, S.; Salmaso, S.; Alexander, C.; Caliceti, P. In Situ Growth of Side-Chain PEG Polymers from Functionalized Human Growth Hormone—A New Technique for Preparation of Enhanced Protein-Polymer Conjugates. *Bioconjugate Chem.* 2010, 21 (4), 671–678. https://doi.org/10.1021/bc900468v.
- (52) Huynh, V.; Ifraimov, N.; Wylie, R. G. Modulating the Thermoresponse of Polymer-Protein Conjugates with Hydrogels for Controlled Release. *Polymers* **2021**, *13* (16), 2772. https://doi.org/10.3390/polym13162772.
- (53) Keefe, A. J.; Jiang, S. Poly(Zwitterionic)Protein Conjugates Offer Increased Stability without Sacrificing Binding Affinity or Bioactivity. *Nature Chem* 2012, 4 (1), 59–63. https://doi.org/10.1038/nchem.1213.
- (54) Han, Y.; Yuan, Z.; Zhang, P.; Jiang, S. Zwitterlation Mitigates Protein Bioactivity Loss in Vitro over PEGylation. *Chem. Sci.* 2018, 9 (45), 8561–8566. https://doi.org/10.1039/C8SC01777H.

- (55) Li, B.; Yuan, Z.; Zhang, P.; Sinclair, A.; Jain, P.; Wu, K.; Tsao, C.; Xie, J.; Hung, H.; Lin, X.; Bai, T.; Jiang, S. Zwitterionic Nanocages Overcome the Efficacy Loss of Biologic Drugs. *Adv. Mater.* 2018, 30 (14), 1705728.
 https://doi.org/10.1002/adma.201705728.
- (56) Li, B.; Yuan, Z.; Jain, P.; Hung, H.-C.; He, Y.; Lin, X.; McMullen, P.; Jiang, S. De Novo Design of Functional Zwitterionic Biomimetic Material for Immunomodulation. *Science Advances* 2020, 6 (22), eaba0754. https://doi.org/10.1126/sciadv.aba0754.
- (57) Liu, S.; Jiang, S. Chemical Conjugation of Zwitterionic Polymers Protects
 Immunogenic Enzyme and Preserves Bioactivity without Polymer-Specific Antibody
 Response. Nano Today 2016, 11 (3), 285–291.
 https://doi.org/10.1016/j.nantod.2016.05.006.
- (58) Lee, P. W.; Isarov, S. A.; Wallat, J. D.; Molugu, S. K.; Shukla, S.; Sun, J. E. P.; Zhang, J.; Zheng, Y.; Lucius Dougherty, M.; Konkolewicz, D.; Stewart, P. L.; Steinmetz, N. F.; Hore, M. J. A.; Pokorski, J. K. Polymer Structure and Conformation Alter the Antigenicity of Virus-like Particle–Polymer Conjugates. *J. Am. Chem. Soc.* 2017, 139 (9), 3312–3315. https://doi.org/10.1021/jacs.6b11643.
- (59) Isarov, S. A.; Lee, P. W.; Pokorski, J. K. "Graft-to" Protein/Polymer Conjugates

 Using Polynorbornene Block Copolymers. *Biomacromolecules* **2016**, *17* (2), 641–648. https://doi.org/10.1021/acs.biomac.5b01582.
- (60) Church, D. C.; Davis, E.; Caparco, A. A.; Takiguchi, L.; Chung, Y. H.; Steinmetz, N. F.; Pokorski, J. K. Polynorbornene-Based Bioconjugates by Aqueous Grafting-from Ring-Opening Metathesis Polymerization Reduce Protein Immunogenicity. *Cell*

- Reports Physical Science **2022**, 3 (10), 101067. https://doi.org/10.1016/j.xcrp.2022.101067.
- (61) Oda, M.; Satta, Y.; Takenaka, O.; Takahata, N. Loss of Urate Oxidase Activity in Hominoids and Its Evolutionary Implications. *Mol Biol Evol* 2002, 19 (5), 640–653. https://doi.org/10.1093/oxfordjournals.molbev.a004123.
- (62) Wu, X. W.; Muzny, D. M.; Lee, C. C.; Caskey, C. T. Two Independent Mutational Events in the Loss of Urate Oxidase during Hominoid Evolution. *J Mol Evol* **1992**, 34 (1), 78–84. https://doi.org/10.1007/BF00163854.
- (63) Naomi Schlesinger, M. D. Diagnosis of Gout: Clinical, Laboratory, and Radiologic Findings. *Supplements and Featured Publications* **2005**, *11* (15 Suppl).
- (64) Mandell, B. F. Clinical Manifestations of Hyperuricemia and Gout. *CCJM* **2008**, *75* (7 suppl 5), S5–S8.
- (65) Girardet, J.-L.; Miner, J. N. Chapter Eleven Urate Crystal Deposition Disease and Gout—New Therapies for an Old Problem. In *Annual Reports in Medicinal Chemistry*; Desai, M. C., Ed.; Academic Press, 2014; Vol. 49, pp 151–164. https://doi.org/10.1016/B978-0-12-800167-7.00011-0.
- (66) Maiuolo, J.; Oppedisano, F.; Gratteri, S.; Muscoli, C.; Mollace, V. Regulation of Uric Acid Metabolism and Excretion. *International Journal of Cardiology* 2016, 213, 8– 14. https://doi.org/10.1016/j.ijcard.2015.08.109.
- (67) Rankin, D. A.; Lowe, A. B. New Well-Defined Polymeric Betaines: First Report Detailing the Synthesis and ROMP of Salt-Responsive Sulfopropylbetaine- and Carboxyethylbetaine-Exo-7-Oxanorbornene Monomers. *Macromolecules* 2008, 41 (3), 614–622. https://doi.org/10.1021/ma701952c.

- (68) Church, D. C.; Pokorski, J. K. Cell Engineering with Functional Poly(Oxanorbornene) Block Copolymers. *Angewandte Chemie International Edition* 2020, 59 (28), 11379–11383. https://doi.org/10.1002/anie.202005148.
- (69) Colak, S.; Tew, G. N. Synthesis and Solution Properties of Norbornene Based Polybetaines. *Macromolecules* 2008, 41 (22), 8436–8440. https://doi.org/10.1021/ma801295u.
- (70) Colak, S.; Tew, G. N. Dual-Functional ROMP-Based Betaines: Effect of Hydrophilicity and Backbone Structure on Nonfouling Properties. *Langmuir* 2012, 28 (1), 666–675. https://doi.org/10.1021/la203683u.
- (71) Izunobi, J. U.; Higginbotham, C. L. Polymer Molecular Weight Analysis by 1H NMR Spectroscopy. J. Chem. Educ. 2011, 88 (8), 1098–1104. https://doi.org/10.1021/ed100461v.
- (72) Wang, Z.; Zhang, Q.; Shen, H.; Yang, P.; Zhou, X. Optimized MALDI-TOF MS Strategy for Characterizing Polymers. *Frontiers in Chemistry* **2021**, *9*.
- (73) Payne, M. E.; Grayson, S. M. Characterization of Synthetic Polymers via Matrix Assisted Laser Desorption Ionization Time of Flight (MALDI-TOF) Mass Spectrometry. *J Vis Exp* 2018, No. 136, 57174. https://doi.org/10.3791/57174.
- (74) Schriemer, D. C.; Li, L. Mass Discrimination in the Analysis of Polydisperse Polymers by MALDI Time-of-Flight Mass Spectrometry. 2. Instrumental Issues. Anal. Chem. 1997, 69 (20), 4176–4183. https://doi.org/10.1021/ac9707794.
- (75) Fields, R. [38] The Rapid Determination of Amino Groups with TNBS. In *Methods in Enzymology*; Enzyme Structure, Part B; Academic Press, 1972; Vol. 25, pp 464–468. https://doi.org/10.1016/S0076-6879(72)25042-X.

- (76) Kurfürst, M. M. Detection and Molecular Weight Determination of Polyethylene Glycol-Modified Hirudin by Staining after Sodium Dodecyl Sulfate-Polyacrylamide Gel Electrophoresis. *Analytical Biochemistry* **1992**, *200* (2), 244–248. https://doi.org/10.1016/0003-2697(92)90460-O.
- (77) Imoto, T.; Yagishita, K. A Simple Activity Measurement of Lysozyme. Agricultural and Biological Chemistry 1971, 35 (7), 1154–1156.
 https://doi.org/10.1080/00021369.1971.10860050.
- (78) Wright, T. A.; Page, R. C.; Konkolewicz, D. Polymer Conjugation of Proteins as a Synthetic Post-Translational Modification to Impact Their Stability and Activity. *Polym. Chem.* **2019**, *10* (4), 434–454. https://doi.org/10.1039/C8PY01399C.
- (79) Lucius, M.; Falatach, R.; McGlone, C.; Makaroff, K.; Danielson, A.; Williams, C.; Nix, J. C.; Konkolewicz, D.; Page, R. C.; Berberich, J. A. Investigating the Impact of Polymer Functional Groups on the Stability and Activity of Lysozyme–Polymer Conjugates. *Biomacromolecules* 2016, 17 (3), 1123–1134. https://doi.org/10.1021/acs.biomac.5b01743.
- (80) Zhang, T.; An, W.; Sun, J.; Duan, F.; Shao, Z.; Zhang, F.; Jiang, T.; Deng, X.; Boyer, C.; Gao, W. N-Terminal Lysozyme Conjugation to a Cationic Polymer Enhances Antimicrobial Activity and Overcomes Antimicrobial Resistance. *Nano Lett.* 2022, 22 (20), 8294–8303. https://doi.org/10.1021/acs.nanolett.2c03160.
- (81) da Silva Freitas, D.; Spencer, P. J.; Vassão, R. C.; Abrahão-Neto, J. Biochemical and Biopharmaceutical Properties of PEGylated Uricase. *International Journal of Pharmaceutics* 2010, 387 (1), 215–222.
 https://doi.org/10.1016/j.ijpharm.2009.11.034.

- (82) Caliceti, P.; Schiavon, O.; Veronese, F. M. Biopharmaceutical Properties of Uricase Conjugated to Neutral and Amphiphilic Polymers. *Bioconjug Chem* **1999**, *10* (4), 638–646. https://doi.org/10.1021/bc980155k.
- (83) Schiavon, O.; Caliceti, P.; Ferruti, P.; Veronese, F. M. Therapeutic Proteins: A Comparison of Chemical and Biological Properties of Uricase Conjugated to Linear or Branched Poly(Ethylene Glycol) and Poly(N-Acryloylmorpholine). *Il Farmaco* 2000, 55 (4), 264–269. https://doi.org/10.1016/S0014-827X(00)00031-8.
- (84) Caliceti, P.; Schiavon, O.; Veronese, F. M. Immunological Properties of Uricase Conjugated to Neutral Soluble Polymers. *Bioconjugate Chem.* **2001**, *12* (4), 515–522. https://doi.org/10.1021/bc000119x.
- (85) Bommarius, A. S.; Paye, M. F. Stabilizing Biocatalysts. *Chem. Soc. Rev.* 2013, 42 (15), 6534–6565. https://doi.org/10.1039/C3CS60137D.
- (86) Caparco, A. A.; Dautel, D. R.; Champion, J. A. Protein Mediated Enzyme Immobilization. Small 2022, 18 (19), 2106425.
 https://doi.org/10.1002/smll.202106425.
- (87) Salmaso, S.; Semenzato, A.; Bersania, S.; Chinol, M.; Paganelli, G.; Caliceti, P. Preparation and Characterization of Active Site Protected Poly(Ethylene Glycol)—Avidin Bioconjugates. *Biochimica et Biophysica Acta (BBA) General Subjects* 2005, 1726 (1), 57–66. https://doi.org/10.1016/j.bbagen.2005.04.025.
- (88) Slütter, B.; Soema, P. C.; Ding, Z.; Verheul, R.; Hennink, W.; Jiskoot, W.
 Conjugation of Ovalbumin to Trimethyl Chitosan Improves Immunogenicity of the
 Antigen. Journal of Controlled Release 2010, 143 (2), 207–214.
 https://doi.org/10.1016/j.jconrel.2010.01.007.

- (89) Pustulka, S. M.; Ling, K.; Pish, S. L.; Champion, J. A. Protein Nanoparticle Charge and Hydrophobicity Govern Protein Corona and Macrophage Uptake. ACS Appl. Mater. Interfaces 2020, 12 (43), 48284–48295. https://doi.org/10.1021/acsami.0c12341.
- (90) Adams, M.; Richmond, V.; Smith, D.; Wang, Y.; Fan, F.; Sokolov, A. P.; Waldow, D. A. Decoupling of Ion Conductivity from Segmental Dynamics in Oligomeric Ethylene Oxide Functionalized Oxanorbornene Dicarboximide Homopolymers.
 Polymer 2017, 116, 218–225. https://doi.org/10.1016/j.polymer.2017.03.054.
- (91) Van Damme, L.; Van Hoorick, J.; Blondeel, P.; Van Vlierberghe, S. Toward Adipose Tissue Engineering Using Thiol-Norbornene Photo-Crosslinkable Gelatin Hydrogels. *Biomacromolecules* 2021, 22 (6), 2408–2418. https://doi.org/10.1021/acs.biomac.1c00189.
- (92) Rodriguez, J.-M. G.; Hux, N. P.; Philips, S. J.; Towns, M. H. Michaelis–Menten Graphs, Lineweaver–Burk Plots, and Reaction Schemes: Investigating Introductory Biochemistry Students' Conceptions of Representations in Enzyme Kinetics. *J. Chem. Educ.* 2019, 96 (9), 1833–1845. https://doi.org/10.1021/acs.jchemed.9b00396.